RSC Advances

PAPER

View Article Online
View Journal | View Issue



Cite this: *RSC Adv.*, 2020, **10**, 42827

# Blends of neem oil based polyesteramide as nanofiber mats to control Culicidae†

Sravanya Konchada,[a] Naresh Killi,[ac] Shahebaz Sayyad,[b] Ganesh B. Gathalkar [bc] and Rathna V. N. Gundloori *[ac]

Mosquitoes act as vectors for several disease-causing microorganisms and pose a threat to mankind by transmitting various diseases. There are different conventional methods to repel or kill these mosquitoes for avoiding susceptibility against infections. However, to overcome the difficulties with conventional methods, new advanced materials are being studied. For the first time, we report developing a nanofiber mat with a controlled release of insecticide to repel or detain the mosquitoes. Briefly, various blend compositions were prepared by manipulating the ratio of neem oil-based polyesteramide (PEA) and polycaprolactone (PCL) immobilized with insecticide, transfluthrin (Tf). The blend solutions were electrospun to get non-woven nanofiber mats, and these nanomaterials were characterized by various spectroscopic techniques to understand their physicochemical properties. The surface morphology was analyzed using environmental scanning electron microscopy (E-SEM), and the diameter of the nanofibers was in the range of 200 to 450 nm. Further, thermal and mechanical properties were evaluated to understand the stability of nanofiber mats. *In vitro* drug release studies of nanofiber mat PPT-1335 showed controlled and sustained release of Tf, with ~35% of Tf released in 24 h. However, a film of the same composition (PPT-1335) showed ~5% of Tf release within 24 h. Moreover, *in vivo* bio-efficacy studies suggested the mortality of mosquitoes was about 50% with PP-133, which was further increased to 100% within 12 h in the presence of Tf (PPT-1335). However, 60% mortality of mosquitoes was observed with the film of PPT-1335. Hence, the nanofiber mat showed better efficacy against mosquitoes as compared to the film of the same composition. The degradation studies under various conditions revealed biocompatibility of the developed nanofiber mats with the ecosystem.

Received 28th September 2020
Accepted 16th November 2020

DOI: 10.1039/d0ra08297j

rsc.li/rsc-advances



## 1. Introduction

Mosquitoes are a group of insects belonging to the family Culicidae with more than 110 genera and subgenera, which include 3600 species making them the most dangerous creatures on the earth. The female mosquitoes feed on the blood of their animal hosts, thus transmitting a wide range of infectious diseases.[1] Further, these mosquitoes act as vectors for many diseases like malaria, filaria, yellow fever, dengue, nile fever, chikungunya, and encephalitis.[2] As a consequence of these diseases, a large number of people lost their lives, which is considered to be more than the wars in history. Most of the African countries are suffering from malaria, and the death rate is around one million for every 200 million cases filed in a year.[3] So, there is a need to control the population of these notorious mosquitoes leading to a variety of diseases. There were several conventional strategies (synthetic or natural repellents, mosquito nets, mosquito traps, electric mosquito zapper, mosquito magnets, *etc.*) to eradicate these mosquito populations for minimizing the number of diseases and their transmission.[4] However, mosquito repellents are extensively used in the form of gels, coils, mats, sticks, sprays, transdermal patches, *etc.*[5] The synthetic chemical components, D-allethrin, D-transallethrin, dimethyl phthalate, transfluthrin, DEET (*N*,*N*-diethyl-*meta*-toluamide), permethrin, piperonyl butoxide, lambda-cyhalothrin, *etc.*[6] were used as mosquito repellents for combating with these mosquitoes.[7,8] Among those insecticides, transfluthrin is mostly used as a mosquito repellent[9,10] which is a pyrethroid insecticide (1*R*-*trans*)-(2,3,5,6-tetrafluorophenyl) methyl-3-(2,2dichloroethenyl)2,2-dimethyl cyclopropane carboxylate. The conventional materials are not that efficient due to the burst release of the insecticides, which leads to environmental pollution and are toxic to human beings.[11] Moreover, in indoors, to release these insecticides from the formulated substrates, mostly heating mechanism is required.[12]

[a]*Polymer Science and Engineering Division, CSIR-National Chemical Laboratory, Dr. Homi Bhabha Road, Pune-411008, Maharashtra, India. E-mail: rv.gundloori@ncl.res.in*

[b]*Laboratory of Entomology, Division of Organic Chemistry, CSIR-National Chemical Laboratory, Dr. Homi Bhabha Road, Pune-411008, Maharashtra, India*

[c]*Academy of Scientific and Innovative Research (AcSIR), Ghaziabad-201002, Uttar Pradesh, India*

† Electronic supplementary information (ESI) available. See DOI: 10.1039/d0ra08297j

Hence, there is always a need for the development of new materials with controlled release of insecticide, which can be used effectively without sacrificing the heat energy and destroying the ecological balance.

For the past several decades, the polymeric materials are being used for the control and sustained release of the active molecules in various fields like tissue engineering scaffolds,[13] drug delivery,[14] wound healing, pest control,[15] *etc.*[16] These materials are either in bulk, micro, and or nanoforms. Selection of the polymers to develop materials depends on desired applications; hence, synthetic and natural polymers are under practice.[17,18] In any area of application, the nanomaterials showed better performance as compared to the bulk materials due to their large surface area with respect to volume, better interaction properties, economic viability, easy handling with improved functionality and activity.[19] Though bulk materials are being investigated, the nanomaterials research for pest control is still in its inception.[20] For example, Abdul Zahir *et al.* tested the efficacy of the insecticide loaded nanoparticles against beetles.[21] Likewise, various nanoparticles were synthesized for their efficacy against arthropod pests, including moths.[22] Learning the nanomaterial properties being more favorable for pest control, significant research on these nanomaterials will be expected. Recently, the versatile nanofibers fabricated using the electrospinning method are being investigated in various fields of applications because of their simplicity in operation, cost-effectiveness, easy to prepare with any combination of polymers and nanocomposites.[23] Moreover, it is easy to immobilize various active molecules in the nanofibers to enhance their efficacy for the respective applications without forfeiting the activity.[24] However, there are no reports on the preparation and utilization of nanofiber mats to control or repel mosquitoes. To surface this knowledge for the said application, we proposed to develop a new nanomaterial using the polymer derived from neem oil.

Neem oil-based polyesteramide (PEA) is being used as antimicrobial material for different applications like coating, tissue engineering due to its antimicrobial property.[25] Moreover, the precursor material of this neem oil-based polymer is considered to be (neem oil) having anti-inflammatory, antifungal, antiseptic, antibacterial, antiviral, antipyretic, antihistamine, anthelmintic, parasiticidal, anti-oxidant and diuretic nature.[26] Further, it is practiced as an emmenagogue, febrifuge, and in herbal beauty treatments, also as insecticides, first aid treatments for numerous skin ailments, topical contraceptives, *etc.*[27] After learning the wide range of properties of neem oil, we anticipated the polymer derived from neem oil and fabricated in the form of a nanofiber mat loaded with Tf would enable the controlled release of Tf to repel or kill the mosquitoes more effectively than the conventional methods. Oil based PEAs have substantial significance because the precursor materials are abundantly available at low cost and are environmentally safe.[28] From the literature survey, there are no suitable examples generated as nanofiber mats against mosquitoes using neem oil based polymers. So, we tried to engender the paths for developing nanomaterials and utilization of neem oil based PEAs. Moreover, PEAs are new class of polymers that have combining properties of both polyesters and polyamides in having good degradation, thermal and mechanical properties.[29] Further, these polymers are capable to link with active agents or other polymers to form hybrid materials.[30] Hence these have better scope to enhance the properties like degradation, thermal stability, high modulus, and tensile strength. Further investigations on PEAs as nanomaterials would improve the properties and enable as controlled release systems for active agents.

Therefore, the present work involves the preparation of various blend compositions with neem oil-based polyesteramide (PEA), and polycaprolactone (PCL) comprising insecticide, transfluthrin (Tf). Fabrication of non-woven nanofiber mats using polymeric blend solutions by electrospinning technique. Analysis of surface morphology, thermal and mechanical properties for the developed nanofiber mats. Evaluation of the efficiency of the developed material for pest control against mosquitoes by *in vitro* drug release studies. Further bio-efficacy and biodegradable studies were monitored.

## 2. Materials and methods

Neem oil, phthalic anhydride, and sodium chloride were purchased from SD Fine Chemicals, India. Sodium methoxide was from Spectrochem Pvt. Ltd., Mumbai, India. Xylene and diethyl ether were from Thomas Baker (Chemicals) Pvt. Ltd., Mumbai, India. Polycaprolactone (PCL), diethanolamine, deuterated chloroform ($CDCl_3$), chloroform were procured from Sigma Aldrich Chemicals, Mumbai, India. Sodium sulphate and sodium bicarbonate were purchased from Merck Ltd, Mumbai, India. Transfluthrin was obtained as a gift sample from the Entomology Division, CSIR-National Chemical Laboratory. All other chemicals and reagents were of analytical grade.

### 2.1 Synthesis of polyesteramide

Neem oil-based polyesteramide was synthesized according to the reported procedure.[25] Briefly, in a 100 mL three-necked flask 11.49 mL of diethanolamine (0.32 g mol) was taken and 0.13 g of sodium methoxide (0.007 g mol) was added and stirred for 1 h at 115 °C in an inert atmosphere using nitrogen gas. After 1 h, 30 mL of neem oil (0.1 g mol) was added dropwise to the reaction mixture using a dropping funnel. Then, the reaction mixture was stirred for another 1.5 h at the same temperature. After completion of the reaction, the reaction mixture was cooled to room temperature and the product was dissolved in diethyl ether. The organic layer was washed with brine solution until the aqueous layer was clear. Later, the organic layer (yellow) was dried with anhydrous sodium sulphate and concentrated using a rotary evaporator to obtain a yellow colored highly viscous compound bis-(2-hydroxy ethyl) neem oil fatty amide (HENA). The intermediate product, 10 g of HENA (0.06 g mol) and 8.46 g of phthalic anhydride (0.06 g mol) were placed in a three necked round bottomed flask and dissolved in 40 mL of xylene, followed by stirring for 30 min for homogenous mixing at room temperature. Later the homogenous solution was refluxed for 6 h at 145 °C. The water formed during the reaction was separated using a Dean–Stark apparatus. The

 

resulting product was diluted with 20 mL of xylene and washed thrice with distilled water. The organic layer was concentrated under reduced pressure to obtain a sticky polymer PEA. The Scheme S1 (ESI†) shows the synthesis of neem oil based PEA.

### 2.2. Preparation of polymeric blend solutions

The individual polymers and their blend solutions were prepared in different compositions using chloroform as a solvent (Table 1). Briefly, the desired concentrations of individual polymers, PCL and PEA, were prepared separately in chloroform. The respective samples were stirred for overnight to obtain a homogenous solution. Further, the individual polymeric solutions were mixed in different ratios to obtain the blend solutions of various concentrations. They were vortexed for 3 h at ambient temperature (25 to 30 °C) for uniform dissolution. To evaluate *in vitro* Tf release and *in vivo* bioefficacy studies, the blend solution containing Tf (5% with respect to total polymer concentration) was prepared by following a similar procedure as explained above, where Tf was added to the blend solution and stirred to attain a homogenous solution. Later, the prepared formulations were subjected to electrospinning for the production of nanofiber mats.

### 2.3. Fabrication of non-woven nanofiber mats by electrospinning technique

A 10 mL plastic syringe with a stainless steel blunt-ended hypodermic needle of diameter 0.8 mm was taken, filled with blend solution either with or without insecticide and fixed on to a syringe pump having provision to control the flow rate of the solution (Model 351, SAGE Instruments, and Division of Orion Research Development). The syringe needle was connected to a high-voltage generator (GAMMA High RR40-3.75/DDPM, voltage regulated DC power supply; Ormond Beach, USA) operated in positive DC mode. An aluminum plate covered with an aluminum foil was used as a collector to deposit the nanofiber. The compositions, as mentioned in Table 1, were fabricated at designated parameters to obtain the nanofiber mats. For instance, the solution flow rate was 0.5 mL $h^{-1}$, the applied voltage was fixed at 15 kV, the distance between the tip of the needle to the collector plate was about 10 cm and the room temperature was maintained at 24 °C.

### 2.4. Degradation studies

The polymers used for the development of nanofiber formulation are biodegradable. To quantify the rate and extent of biodegradation of the nanofiber mats, the degradation studies were carried out by exposing them to the soil, water and enzymatic conditions.[31] For these studies, the nanofiber mats were cut into small pieces of 5 mg size and the experimental protocols were followed using the respective samples in triplicates.

**Soil degradation.** The known weights of the nanofiber mats (10 × 10 mm) of the composition (PCL-13, PP-133 and PPT-1335) were taken in triplicates and placed in a Petri dish. These were buried in the soil and exposed to environmental conditions. The humidity was maintained by spraying water in the soil and after a certain period of time, these mats were removed and washed with deionized distilled water. These were dried under vacuum at 30 °C for constant weight and the percentage of weight loss was studied. The percentage of weight loss was given by the following equation.

$$\text{The percentage of weight loss (\%)} = \frac{\text{initial weight of the mat} - \text{final weight of the mat}}{\text{initial weight of the mat}} \times 100$$

**Hydrolytic degradation (water).** The nanofiber mats of blend compositions (PCL-13, PP-133 and PPT-1335) were taken in triplicates and were cut into 10 × 10 mm in size. The samples were transferred to their respective vials containing 10 mL phosphate buffer and were left at 37 °C, regulated by a thermostatically controlled chamber. After five days, the individual nanofiber mats were removed, washed with deionized water and dried under a vacuum at 30 °C. The dried fibers were weighed and the degree of biodegradation was estimated from the percentage of weight loss after hydrolytic degradation. The E-SEM images of the degraded samples were also taken to visualize the effect of degradation on the morphology of the fibers. The hydrolytic degradation studies were done at different pH, 7.4 and 11.8.

**Enzymatic degradation.** Similarly, the nanofiber mats of the compositions (PCL-13, PP-133 and PPT-1335) were cut into 10 × 10 mm in triplicates. The samples were taken in a sample vial containing 10 mL phosphate buffer solution (pH 7.2) with an esterase enzyme (100 μg $mL^{-1}$). These samples were incubated at 37 °C for 5 days to undergo enzymatic degradation.

Table 1 Formulations of pure PCL blend compositions of PCL/PEA with and without insecticide for electrospinning

| PCL (wt/v%) | PEA (wt/v%) | Tf (wt/wt%) w. r. t. total polymer concentration | Composition/formulation code |
|---|---|---|---|
| 8 | — | — | PCL-8 |
| 10 | — | — | PCL-10 |
| 13 | — | — | PCL-13 |
| 13 | 1 | — | PP-131 |
| 13 | 2 | — | PP-132 |
| 13 | 3 | — | PP-133 |
| **13** | **3** | **5** | **PPT-1335** |

Phosphate buffer solution without enzyme was used as a control. After a certain interval of time, the respective nanofiber mats were taken out, washed with deionized water and dried under vacuum at 30 °C to a constant weight.

Further, the surface morphology of the degraded nanofiber mats was evaluated by E-SEM to understand the change in morphology of the nanofiber mats.

### 2.5. *In vitro* Tf release studies

The insecticidal release was estimated using the standard curve of the insecticide, Tf. The Tf loaded nanofiber mat and film were cut into small pieces of 5 mg each, then placed in 5 mL sample vial. The release studies of Tf for each composition were done in triplicates to minimize the error. After a particular time interval, the mats were removed and transferred into the consecutive vials, which corresponds to the next time interval. The Tf released in the first interval was extracted by adding 2 mL of chloroform for recording the optical density (OD) at a $\lambda_{max}$ 271 nm and was extrapolated for the amount released using the standard curve of Tf. This protocol was continued at regular intervals, over a period of 24 h. The percent of Tf released was estimated using eqn (1).

$$\text{Percent of cumulative Tf released } (\%) = \frac{\text{concentration of drug released at time } t}{\text{total concentration of drug loaded in the nanofiber mat}} \times 100 \quad (1)$$

### 2.6. Bio-efficacy studies

Surface bio-efficacy studies were performed on a rectangular white tile (30 × 30 cm) against the mosquito breed, *Aedes aegypti*. The mosquito species were reared in the Entomology Division of CSIR-National Chemical Laboratory, at 25–27 °C and 60–70% relative humidity. Larvae of all stages were nourished with rabbit feed and yeast powder. Adult mosquitoes were fed with 20% sucrose solution and for bioassay studies, those mosquitoes of two to five days old female mosquitoes ($n = 10$) per replicate were used. A square piece (2 × 2 cm) of nanofiber mat of PCL-13, PP-133, PPT-1335 and film of PPT-1335 were taken and placed on the respective rectangular tiles. Nanofiber mat of PCL-13 was used as control. Glass funnels of 12.5 cm in diameter were inverted on the surface of the tiles containing the pieces of samples. In continuation, the test mosquitoes were released through the top opening of the inverted funnel in particular numbers ($n = 10$) and the funnels were plugged with cotton balls. Later, the behavior of these mosquitoes was observed for various time intervals, 1, 2, 4, 6, 8, 12 and 24 h. Initially, the observations were made for every 5 min up to 0.5 h and later for every hour up to 24 h. The number of mosquitoes knocked down were counted with respect to the time intervals. Further, to understand the post-treatment, both the knocked down and the alive mosquitoes were collected in recovery jar and provided with 20% sucrose solution to monitor the survival and mortality rate after 24 h.[32]

## 3. Characterization

Functional characteristics of the pure polymers and nanofiber mats with and without Tf were analyzed using Fourier Transform Infrared Spectrometer (FT-IR) (Perkin Elmer Spectrometer I, FT-IR diffused reflectance mode (DRIFT) mode, USA). Wavenumber of the FT-IR spectrum was recorded, ranging from 4000–500 $cm^{-1}$ with a resolution of 4 $cm^{-1}$ and 8 scans. The surface morphology of the developed nanofiber mats was evaluated using E-SEM model Quanta 200 3D, Dual-beam SEM. The sample for the SEM analysis was prepared by taking the respective piece of the sample (PCL-13, PP-133, PPT-1335, and film of PPT-1335) and mounted on the sample stub using carbon tape. For E-SEM analysis, the nanofiber mats were sputtered with gold using FEI USA coating unit to make samples conductive. The mounted stub was analyzed for surface morphology by E-SEM whose electron source was tungsten (W) filament and with a resolution of 3 nm. Thermal analysis of the nanofiber mats was performed using differential scanning calorimetry (Model Q10 DSC, TA instrument, New Castle, DE, USA). To record the thermogram of a sample, 2–5 mg of the respective sample was weighed in DSC pan and was sealed by applying pressure and exposed to three cycles of heating and cooling. The respective sample was equilibrated to −70 °C for 2 min. In the first cycle, the sample was heated to 200 °C at a ramp of 10 °C $min^{-1}$. In the second cycle, it was quenched to −70 °C and in the third cycle, it was heated to 250 °C at 5 °C ramp per min. A similar method was followed for all the samples. The mechanical strength of the developed nanofiber mats was analyzed using a dynamic mechanical analyzer, Rheometrics Solids Analyzer in tension mode (RSA-III), TA Instruments, USA. The respective nanofiber mats were cut into rectangular strips of 20 × 0.5 cm in size and each of it was loaded onto the tensile grips using a torque meter. The strain rate was fixed to 10 mm $min^{-1}$ and the gauge length to 15 cm. Each sample of the same composition was tested five times to confirm its reproducibility in attaining stress–strain curves. The crystallinity of the polymers before and after fabricating the nanofiber mats were evaluated with a Rigaku X-ray diffractometer model, $D_{max}$ 2500 with Cu K$\alpha_1$ (0.154 nm) radiation operated at 40 kV and 100 mA. The sample was scanned in the $2\theta$ range of 5–40°. Tf estimation and Tf release studies were performed using UV 1601PC UV spectrophotometer (Shimadzu, Japan).

## 4. Results and discussion

In this study, we designed blends of PEA and fabricated the nonwoven nanofiber mats with and without Tf to evaluate their

 

potential for controlling the mosquitoes. Polyesteramide being a low molecular weight polymer of ~12 000 Da, is incapable of producing nanofibers.[33] Hence, it was blended with FDA approved polymer, PCL of molecular weight ~60 000 Da. Various blend compositions were prepared to fabricate non-woven nanofiber mats by electrospinning technique. Several trial experiments were done to produce smooth nanofibers using various concentrations of PCL, where PCL of 13% (PCL-13) was confirmed to be suitable for the production of nanofibers. Accordingly, different compositions of PCL with PEA were prepared as listed in Table 1. Among the various compositions prepared, PP-133 was suitable for loading the Tf. The surface morphology of the nanofiber mats was analyzed and the morphology of the respective compositions are shown in Fig. 1. The morphology of PCL-8, PCL-10 showed the presence of beads in the mat (Fig. 1a and b), whereas, for PCL-13 composition, smooth and continuous fibers were obtained (Fig. 1c). The diameter of the nanofibers ranged from 200 to 250 nm. Further, Fig. 1d, e and f showed the surface morphology of PP-131, PP-132 and PP-133, respectively. The diameter of the nanofibers for these compositions increased from 250 to 350 nm, which was directly proportional to the increase in the concentration of PEA in the blend composition. Similarly, the morphology of the nanofiber mats with insecticide (Tf), PPT-1335 (Fig. 1g), revealed a marginal increase in diameter ranging from 300 to 450 nm with an increase in the addition of Tf. Further, a film (PPTF-1335) was prepared by the solution casting method with the composition of PPT-1335 to compare the performance of the nanofiber mat (PPT-1335) of the same composition. Fig. 1d shows the surface morphology of the film, which contains numerous small pores in it.

The interactions between the active agent and the polymers of the nanofiber mats and their functional characteristics were analyzed using FT-IR spectroscopy. Fig. 2 shows the infrared spectrum of pure polymers PCL, PEA and nanofiber mats of compositions, PP-133, PPT-1335. The FT-IR spectra of PCL-13 showed the characteristic peaks of pure PCL at 2931 $cm^{-1}$, which is due to asymmetric and symmetric H–C– stretching in alkenes, a carbonyl stretching (C═O) peak of ester bond at 1738 $cm^{-1}$. The synthesized polyesteramide (PEA) showed characteristic peaks at 3430 $cm^{-1}$ due to the alcoholic OH group, 2925 $cm^{-1}$ for H–C– stretching, 1732 $cm^{-1}$ due to –COOC– ester group and a peak at 1660 $cm^{-1}$ due to amide groups. Further, the FT-IR spectra of Tf recorded the characteristic peaks at 3023 $cm^{-1}$ and 1726 $cm^{-1}$ due to H–C– stretching and ester group, respectively. Multiple peaks appeared at 1640, 1535 and 1450 $cm^{-1}$ due to C═C in alkenes. The FT-IR spectra of blend composition, PP-133 showed the characteristic peaks of all the polymers at 3503 $cm^{-1}$ due to alcoholic OH group, 2907 $cm^{-1}$ for H–C– stretching, 1720 $cm^{-1}$ due to ester group –COOC and a peak at 1665 $cm^{-1}$ –NHCO due to amide group indicating the presence of PEA and PCL. Similarly, the Tf loaded blend composition, PPT-1335, recorded a peak at 1208 $cm^{-1}$ due to the presence of Tf, in addition to the peaks of the respective polymers (3455 $cm^{-1}$, 2925 $cm^{-1}$, 1726 $cm^{-1}$ and 1670 $cm^{-1}$). The shifting of peaks in the spectra

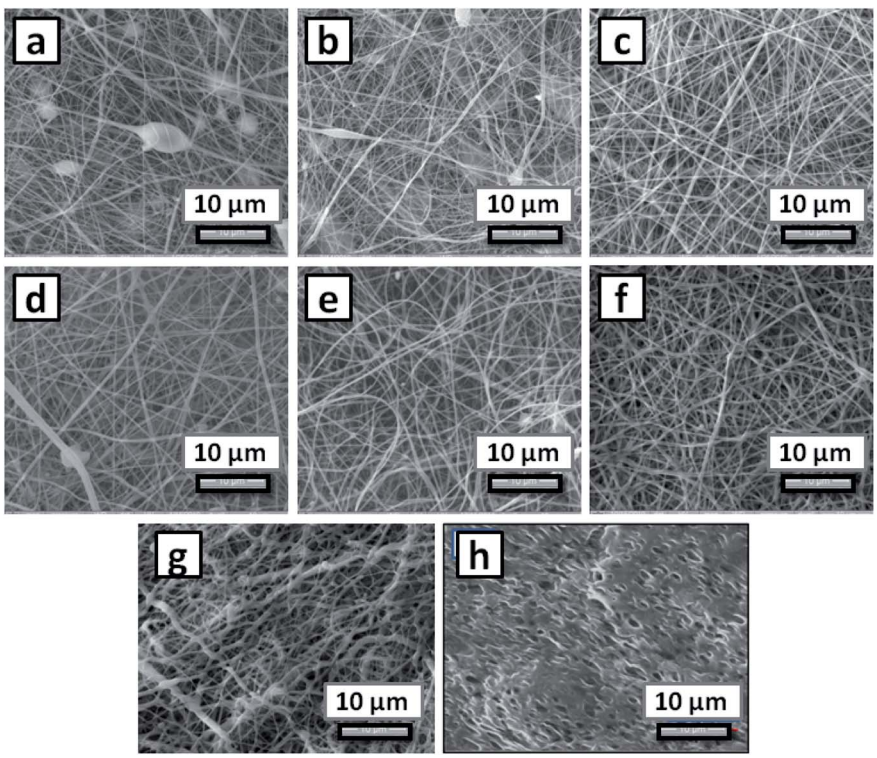


Fig. 1 Surface morphology of electrospun nanofiber mats; (a) PCL-8, (b) PCL-10, (c) PCL-13, (d) PP-131, (e) PP-132, (f) PP-133, (g) PPT-1335 and (h) PPTF-1335.

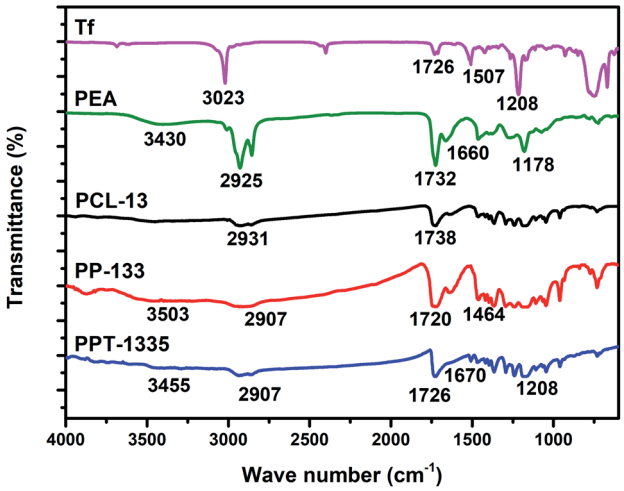


Fig. 2 FT-IR spectra of Tf, PEA, PCL-13, PP-133 and PPT-1335.

of the blends of nanofiber mats with and without Tf was attributed to the hydrogen ion interactions between the polymers and the insecticide, Tf.

Differential scanning calorimetry (DSC) technique is used for analyzing the thermal properties of the pure polymers and nanofiber mats prepared from polymer blend compositions (Fig. 3). The thermogram of pure PCL nanofiber mat (PCL-13) recorded glass transition temperature ($T_g$) and melting temperature ($T_m$) at −58 and 56 °C respectively, these values were similar to the reported literature ($T_g$, −60 and $T_m$, 60 °C).[34] Further, the thermogram of PEA recorded $T_g$ and $T_m$ at −13 and 58 °C, respectively. The nanofiber of blend composition, PP-133, recorded $T_g$ at −58 °C and $T_m$ at 56 °C, reflecting the presence of PCL. However, no new $T_g$ or $T_m$ were recorded, which indicates the blend is homogenous without phase separation.

Fig. 3 shows the $T_g$ and $T_m$ values of the PCL-13 nanofiber mat recorded. These values are suggesting the nano-formulations of bulk PCL to nano-sized PCL. Thermogram of blend composition, PPT-1335, recorded $T_g$ and $T_m$ at −44.8 and 58.7 °C, respectively. The shifting of $T_g$ and $T_m$ of the blend composition, PPT-1335, is due to the interaction between the polymer and the Tf.

X-ray diffractograms were recorded for the nanofiber mats of PCL-13, PP-133 and PPT-1335 (Fig. 4). These studies were done to investigate the changes in the crystallinity of the nanofiber mats before and after blending with PEA and Tf. XRD pattern of PCL-13 nanofiber mat recorded two broad semi-crystalline peaks at 2$\theta$ of 21.3° and 23.6°, which were similar to that of pure PCL (2$\theta$ of 21.9° and 24.3°).[35] X-ray diffractogram of PP-133 nanofiber mat recorded low-intensity peaks at 2$\theta$ of 21.7° and 24.1°, which is caused due to the blending of PCL with amorphous PEA. Further, the addition of Tf to the blends of PCL and PEA enabled an additional reduction in the intensity of the crystalline peaks of PCL. Therefore, it was understood that the PPT-1335 nanofiber mat is more amorphous (2$\theta$ 21.8° and 24.3°). These results indicated that the blend compositions were homogenous and non-phase separated.

Nanofiber mats with good mechanical strength are desirable to sustain practical applications. Hence, we evaluated the

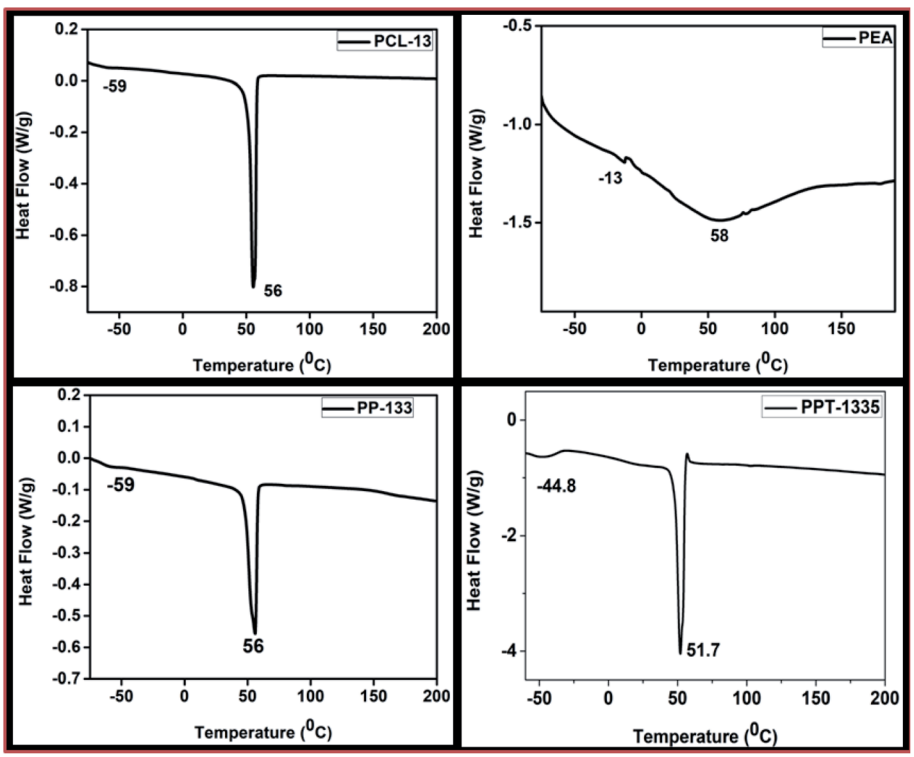


Fig. 3 DSC graphs of PCL-13, PEA, PP-133 and PPT-1335.

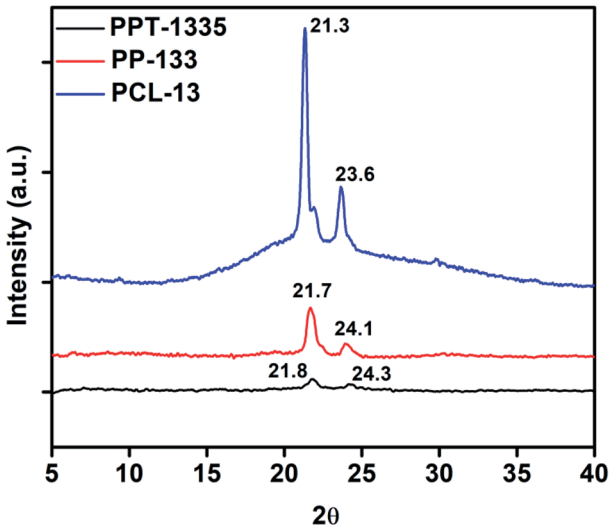


Fig. 4 Powder XRD spectra of nanofiber mats, PCL-13, PP-133 and PPT-1335.

mechanical strength of the electrospun nanofiber mats. Accordingly, the stress–strain experiments were recorded and plotted graphs to cognize the tensile strength and modulus of the nanofiber mats before and after blending with PEA and Tf. Fig. 5 depicts the stress–strain curves of PCL-13, PP-133, and PPT-1335 nanofiber mats. The tensile strength of the PCL nanofiber mat was 0.39 MPa and its modulus was recorded to be 0.195 MPa. The tensile strength and modulus of blend composition; PP-133 was 2.64 MPa and Young's modulus was 0.658 MPa, respectively. From this data, it is understood that PCL nanofiber mats are less in mechanical strength when compared to the nanofiber mats of the blend (PP-133), which showed 88% more strength than that of the PCL nanofiber mats. The increase in both the tensile strength and modulus values of the PP-133 nanofiber mat was attributed to the presence of polyesteramide. It is well illustrated that the amide bond present in the backbone of polyesteramide is responsible for improvising the flexibility and strength of the nanofibers.[36] Also, the nanofiber mats with insecticide sustained good modulus equal to 0.3 MPa and tensile strength equal to 1.88 MPa because of the interactions between the insecticide and polymers. The interactions between the polymers and Tf were confirmed from XRD and DSC studies.

Degradation of the developed nanofiber mats (PCL-13, PP-133 and PPT-1335) were studied in the presence of water, enzyme and soil separately. The method to degrade these materials was explained in the Experimental section (Materials and methods, 2.4). As per the protocol, 5 mg of nanofiber mats were subjected to different conditions like hydrolytic, enzymatic and soil for a particular period of time (5 days) and the degradation rates were calculated in terms of weight loss of the degraded nanofiber mats. Fig. 6 exhibits the percentage of weight loss of the nanofiber mats under various conditions and from the contour, it is evident that the maximum degradation is recorded for the samples, which were imperiled through the enzyme as compared to the mats subjected to other conditions. The enzyme esterase cleaved the peptide and ester bonds present in PCL, PEA more efficiently. Further, it was noticed that the degradation of soil conditions too showed noticeable degradation, which was comparable to enzymatic degradation. The percentage of weight loss of the nanofiber mat (PPT-1335) was 22% and 16% by enzymatic and soil degradation, respectively. However, the hydrolytic degradation of the nanofiber mat at the end of the 5th day was 15%. Finally, we conclude that the rate of degradation rate was enhanced for the blend compositions (PP-133 and PPT-1335) due to the presence of ester and amide bonds in PEA.

Further, to understand the surface morphology after degradation, E-SEM studies were done. Fig. 7 shows the morphology of the respective nanofiber mats after exposure to the various methods, as explained above. The morphology of the nanofiber mats was different as compared to the non-degraded nanofiber mats. The nanofibers appeared to be discontinuous in case of enzymatic and soil degradation, the number and the size of the pores increased and the diameter decreased to some extent. However, in the hydrolytic degradation (H1, H2 and H3), there are no significant changes in the morphology of the nanofiber mats. From these results, we can clearly say that the developed nanofiber mats are biodegradable, as the components used are FDA approved polymers. Therefore the degraded fragments are considered to be environmentally safe.

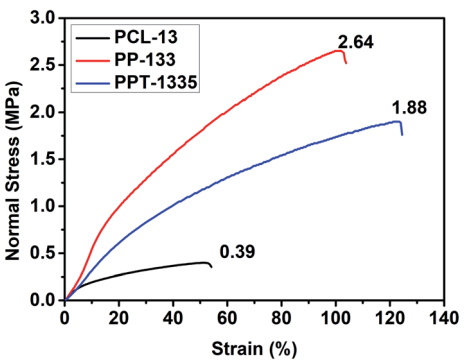


Fig. 5 Stress *vs.* strain curves of nanofiber mats, PCL-13, PP-133 and PPT-1335.

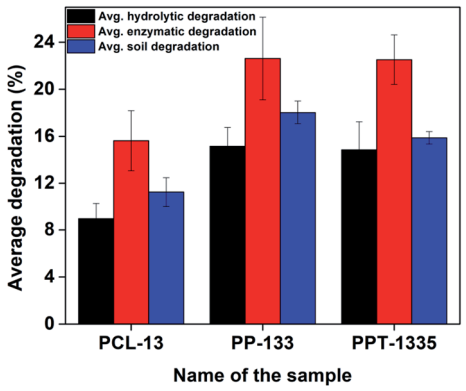


Fig. 6 The percent of weight loss of the nanofiber mats of PCL-13, PP-133 and PPT-1335.

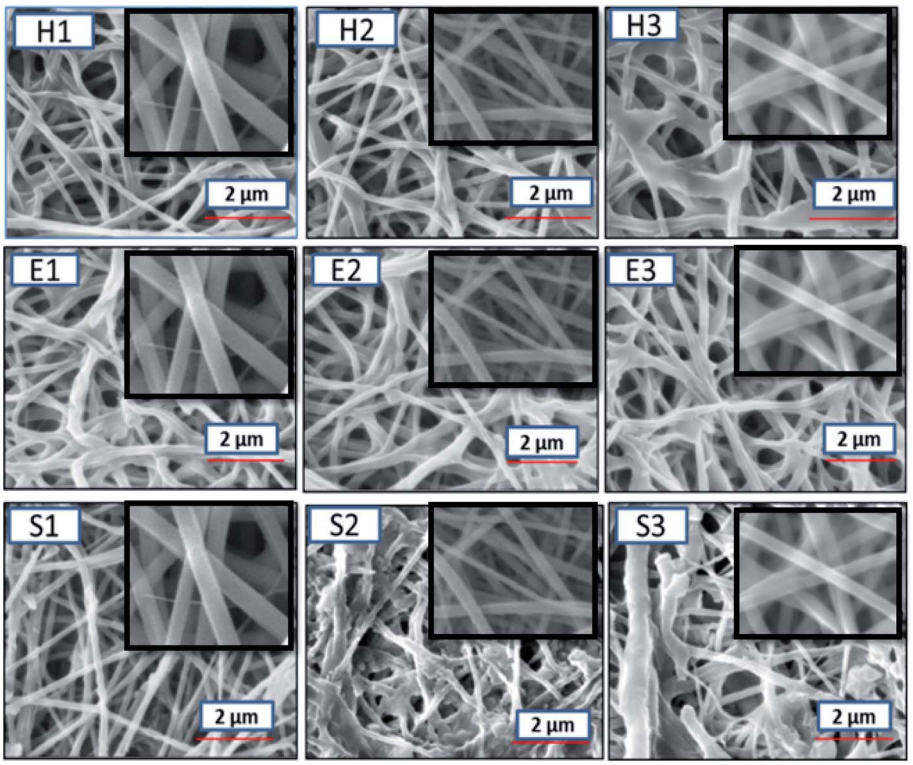


Fig. 7 E-SEM images of the degraded nanofiber mats (1) PCL-13, (2) PP-133 and (3) PP-1335 (inset shows the E-SEM images of non-degraded nanofibers) where H – hydrolytic degradation, E – enzymatic degradation and S – degradation in soil.

*In vitro*, Tf release studies were performed for the developed nanofiber mats loaded with Tf in order to estimate the drug release from the nanofiber mats at different time intervals. The protocol for the release of Tf from the nanofiber mats was explained in the Experimental section (2.5). The nanofiber mats were compared with films (bulk material) of the same composition (PPT-1335) using Tf release data for over a period of time to understand the efficacy for the desired application. Fig. 8 shows the insecticidal release curve as a function of time for the Tf loaded nanofiber mat and film. The Tf released from the nanofiber mat was recorded for 24 h. Initially for 1 h, 8% of Tf was released and subsequently there was a gradual increase in the percent of release with time. After 24 h, the cumulative Tf release from the nanofiber mat, PPT-1335 was 33%. On the other hand, 2% of Tf was release in 1 h from the film, PPTF-1335 and after 24 h ~5% of Tf was released. As anticipated, the release of Tf from the nanofiber mat was significant as compared to the film due to high surface area of the nanofibers, as a result there was more diffusion of Tf.[37] Further there was no burst release recorded from the nanofiber mats.

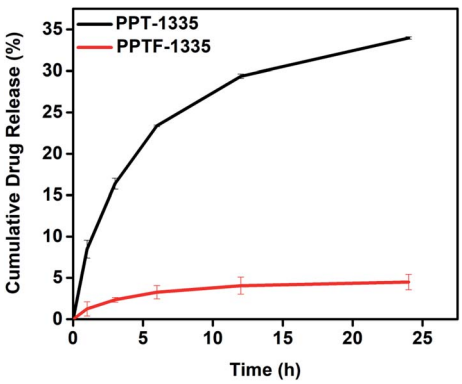


Fig. 8 *In vitro* Tf release of nanofiber mat (PPT-1335) and film prepared using blend composition of PPT-1335 (PPTF-1335).

For supporting the above release data, we performed the quantification studies using an advanced technique, gas chromatography/mass spectrometry (GC-MS). The details of materials and methods were explained in the ESI, page no. (S3–S6†). The concentration of Tf released from the blend compositions, PPT-1335 and PPTF-1335, were analyzed quantitatively for 12 h. The release of Tf from the nanofiber mat was about 19.2%, whereas the film of the same composition showed 8% of release after 12 h. These results suggested that the nanofiber mat (PPT-1335) showed greater efficiency towards Tf release as compared to the film (PPTF-1335) of the same composition. The quantification of Tf was recorded using standard curve of Tf by GC-MS as shown in Fig. S4 (ESI†).

*In vitro* bio-efficacy studies were performed against the mosquitoes, *Aedes aegypti* using nanofiber mats of compositions, PCL-13, PP-133, PPT-1335 and PPTF-1335. These studies were performed at room temperature using replicates of five samples each to minimize the errors in the result. The methodology of the bioefficacy studies was explained in Section 2.6. We have recorded the number of mosquitoes knocked down

 

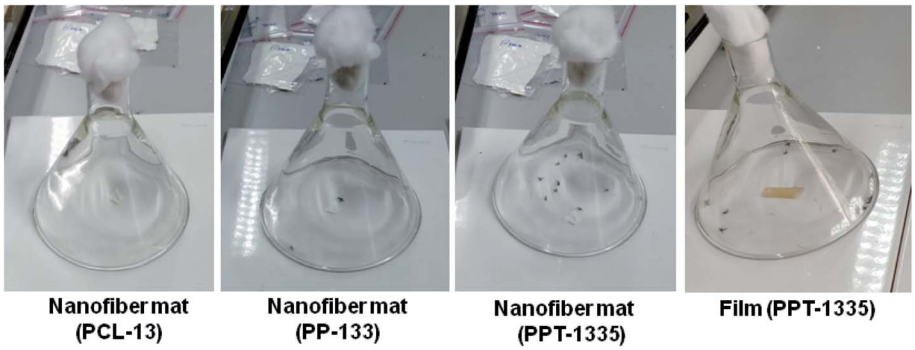


Fig. 9 Images of bio-efficacy studies of nanofiber mats of PCL-13, PP-133, PPT-1335 and film, PPTF-1335.

using respective test samples with the function of time. Fig. 9 shows the images of mosquitoes knocked down with nanofiber mat of PCL-13, PP-133, PPT-1335 and film, PPTF-1335. After 12 h, we observed, 100% knock down of mosquitoes in the presence of nanofiber mat, PPT-1335. However, at the same time, 30% and 60% of mosquitoes were knocked down with the nanofiber mat without Tf (PP-133) and film, PPTF-1335, respectively. A nanofiber mat of PCL-13 was used as a control, where we observed zero knock downs of mosquitoes for 24 h. After every time interval of observation, the mosquitoes that were knockdown and alive were collected in a recovery jar and fed with appropriate food and water to monitor the survival and mortality of the mosquitoes (Table 2).

The average percentage of the mortality of mosquitoes was shown in Table 2. The blend composition of PP-133 nanofiber mat showed 10, 30 and 50% of mortality for 8, 12 and 24 h respectively due to the presence of bioactive neem oil-based PEA. Further, the mortality of mosquitoes was increased by the addition of insecticide (Tf) in the nanofiber mat (PPT-1335), which was 10, 50, 80 and 100% at 2, 4, 8 and 12 h respectively. However, the mortality with film, PPTF-1335 was 10, 30, 60 and 100% at 2, 4, 8, 12 and 24 h respectively because of prolonged release of Tf. It is noteworthy that 100% mortality was observed at 12 h with the nanofiber mat of PPT-1335, whereas; the film of the same composition took 24 h to record 100% of mortality. However, as expected, the nanofiber mat of PCL-13 did not show any mortality rate of mosquitoes even after 24 h as it is not bioactive. From the overall observation, we concluded that the developed nanofiber mats are more efficient for controlling mosquitoes and hence can be recommended for further studies.

Table 2 Percentage of mortality of mosquitoes with the nanofiber mats of PCL-13, PP-133, PPT-1335 and film, PPTF-1335

| | Percentage of mortality of mosquitoes at a time (%) | | | | | |
|---|---|---|---|---|---|---|
| Composition name | 1 h | 2 h | 4 h | 8 h | 12 h | 24 h |
| Nanofiber mat, PCL-13 | 0 | 0 | 0 | 0 | 0 | 0 |
| Nanofiber mat, PP-133 | 0 | 0 | 0 | 10 | 30 | 50 |
| Nanofiber mat, PPT-1335 | 0 | 10 | 50 | 80 | 100 | — |
| Film, PPTF-1335 | 0 | 0 | 10 | 30 | 60 | 100 |

## 5. Conclusion

Nanofiber mats are being studied for various applications; however, very seldom research is reported on the applicability of nanofiber mats as repellants to control mosquitoes. In these studies, we were successful in designing nanofiber mats using neem oil-based polyesteramides immobilized with insecticide, Tf. As anticipated, the developed nanofiber mats were more efficient than the films because there was a direct relationship between size and activity. For the practical application of the nanofiber mats, it is desirable to know whether the mats are stable mechanically. The mechanical studies of the nanofiber mats with and without Tf were more efficient than the nanofiber mats of PCL, indicating their stability to withstand weathering or handling conditions. Further, the nanofiber mats were thermally stable up to 200 °C so, exposure to heat or shelf life is not at stake. *In vitro* release of Tf from nanofiber mats was 35%, whereas films of the same composition (PPTF-1335) recorded 5% release for 24 h. From the release data, it was observed that the rate and amount of Tf release was faster from nanofiber mats and was adequate to control the mosquitoes than the films. Hence, the total number of knocked down mosquitoes were 100% within 12 h of time for the nanofiber mat, however, the films took 24 h for the same. To value the developed nanomaterials as non-pollutants, the biodegradation studies were evaluated under various conditions. The maximum degradation rate for the nanofiber mats under enzymatic conditions was recorded as 22%, which was due to degradation of ester and amide linkage. This was confirmed by the appearance of the discontinuous nanofibers and the formation of large pores in the morphology (E-SEM). The chemical and physical properties of nanofiber mats with Tf being more favorable than the conventional materials, so the developed nanofiber mats would be preferable to control the mosquitoes.

## Conflicts of interest

There are no conflicts to declare.

## Acknowledgements

The authors are grateful to the funding agencies, CSIR (MLP034726), New Delhi, BIRAC (GAP327326) and CSIR-SRF, New Delhi. The authors also are thankful to Dr H. V. Thulasiram and Mr Shrikant Karegaonkar for their support in quantification studies by GC-MS.

## References

1 B. Breedlove and P. M. Arguin, Hematophagous Endeavors, Fact and Fancy, *Emerging Infect. Dis.*, 2017, **23**(8), 1436–1437.
2 M. S. Mulla, U. Thavara, A. Tawatsin, W. Kong-Ngamsuk and J. Chompoosri, Mosquito burden and impact on the poor: Measures and costs for personal protection in some communities in Thailand, *J. Am. Mosq. Control Assoc.*, 2001, **17**(3), 153–159.
3 N. Kuntworbe, N. Martini, J. Shaw and R. Al-Kassas, Malaria Intervention Policies and Pharmaceutical Nanotechnology as a Potential Tool for Malaria Management, *Drug Dev. Res.*, 2012, **73**(4), 167–184.
4 T. Ahmed, M. Z. Hyder, I. Liaqat and M. Scholz, Climatic Conditions: Conventional and Nanotechnology-Based Methods for the Control of Mosquito Vectors Causing Human Health Issues, *Int. J. Environ. Res. Public Health*, 2019, **16**(3165), 1–25.
5 M. Naz, N. Rehman, M. Nazam Ansari, M. Kamal, M. A. Ganaie, A. S. Awaad and S. I. Alqasoumi, Comparative study of subchronic toxicities of mosquito repellents (coils, mats and liquids) on vital organs in Swiss albino mice, *Saudi Pharm. J.*, 2019, **27**(3), 348–353.
6 G. Benelli, Research in mosquito control: current challenges for a brighter future, *Parasitol. Res.*, 2015, **114**(8), 2801–2805.
7 E. Panagiotakopulu, P. C. Buckland, P. M. Day, A. A. Sarpaki and C. Doumas, Natural Insecticides and Insect Repellents in Antiquity – a Review of the Evidence, *J. Archaeol. Sci.*, 1995, **22**(5), 705–710.
8 S. J. Peter, M. J. Miller, A. W. Yasko, M. J. Yaszemski and A. G. Mikos, Polymer concepts in tissue engineering, *J. Biomed. Mater. Res.*, 1998, **43**(4), 422–427.
9 T. Katz, J. Miller and A. Hebert, Insect repellents: Historical perspectives and new developments, *J. Am. Acad. Dermatol.*, 2007, **56**(2), Ab53.
10 T. M. Katz, J. H. Miller and A. A. Hebert, Insect repellents: Historical perspectives and new developments, *J. Am. Acad. Dermatol.*, 2008, **58**(5), 865–871.
11 V. P. Sharma, Health hazards of mosquito repellents and safe alternatives, *Curr. Sci. India*, 2001, **80**(3), 341–343.
12 J. C. Dickens and J. D. Bohbot, Mini review: Mode of action of mosquito repellents, *Pestic. Biochem. Physiol.*, 2013, **106**(3), 149–155.
13 S. Bhagyashri, T. Gadgil, N. Killi and G. V. N. Rathna, Polyhydroxyalkanoates as biomaterials, *Medchemcomm*, 2017, **8**(9), 1774–1787.
14 N. Killi, R. A. Dhakare, A. Singam, M. Lokanadham, H. Chitikeshi and R. V. N. Gundloori, Design and fabrication of mechanically strong nano-matrices of linseed oil based polyesteramide blends, *Medchemcomm*, 2016, **7**(12), 2299–2308.
15 A. Roy, S. K. Singh, J. Bajpai and A. K. Bajpai, Controlled pesticide release from biodegradable polymers, *Cent. Eur. J. Chem.*, 2014, **12**(4), 453–469.
16 S. Ramakrishna, J. Mayer, E. Wintermantel and K. W. Leong, Biomedical applications of polymer-composite materials: a review, *Compos. Sci. Technol.*, 2001, **61**(9), 1189–1224.
17 M. Lapointe and B. Barbeau, Understanding the roles and characterizing the intrinsic properties of synthetic vs. natural polymers to improve clarification through interparticle Bridging: A review, *Sep. Purif. Technol.*, 2020, 231.
18 M. R. Sanjay, P. Madhu, M. Jawaid, P. Senthamaraikannan, S. Senthil and S. Pradeep, Characterization and properties of natural fiber polymer composites: A comprehensive review, *J. Cleaner Prod.*, 2018, **172**, 566–581.
19 G. Guisbiers, S. Mejia-Rosales and F. L. Deepak, Nanomaterial Properties: Size and Shape Dependencies, *J. Nanomater.*, 2012, **2012**, 1–2.
20 T. Jana, B. C. Roy and S. Maiti, Biodegradable film 6. Modification of the film for control release of insecticides, *Eur. Polym. J.*, 2001, **37**(4), 861–864.
21 A. A. Zahir and A. A. Rahuman, Evaluation of different extracts and synthesised silver nanoparticles from leaves of *Euphorbia prostrata* against *Haemaphysalis bispinosa* and *Hippobosca maculata*, *Vet. Parasitol.*, 2012, **187**(3–4), 511–520.
22 (*a*) G. Benelli, Green synthesized nanoparticles in the fight against mosquito-borne diseases and cancer – a brief review, *Enzyme Microb. Technol.*, 2016, **95**, 58–68; (*b*) Y. Liu, Z. Tong and R. K. Prud'homme, Stabilized polymeric nanoparticles for controlled and efficient release of bifenthrin, *Pest Manage. Sci.*, 2008, **64**(8), 808–812; (*c*) F. L. Yang, X. G. Li, F. Zhu and C. L. Lei, Structural Characterization of Nanoparticles Loaded with Garlic Essential Oil and Their Insecticidal Activity against *Tribolium castaneum* (Herbst) (Coleoptera: Tenebrionidae), *J. Agric. Food Chem.*, 2009, **57**(21), 10156–10162.
23 J. J. Xue, T. Wu, Y. Q. Dai and Y. N. Xia, Electrospinning and Electrospun Nanofibers: Methods, Materials, and Applications, *Chem. Rev.*, 2019, **119**(8), 5298–5415.
24 S. Kumar, M. Nehra, N. Dilbaghi, G. Marrazza, A. A. Hassan and K. H. Kim, Nano-based smart pesticide formulations: Emerging opportunities for agriculture, *J. Controlled Release*, 2019, **294**, 131–153.
25 A. B. Chaudhari, P. D. Tatiya, R. K. Hedaoo, R. D. Kulkarni and V. V. Gite, Polyurethane Prepared from Neem Oil Polyesteramides for Self-Healing Anticorrosive Coatings, *Ind. Eng. Chem. Res.*, 2013, **52**(30), 10189–10197.
26 J. Jerobin, P. Makwana, R. S. Suresh Kumar, R. Sundaramoorthy, A. Mukherjee and N. Chandrasekaran, Antibacterial activity of neem nanoemulsion and its toxicity assessment on human lymphocytes in vitro, *Int. J. Nanomed.*, 2015, **10**(Suppl 1), 77–86.

 

27 E. V. R. Campos, J. L. de Oliveira, M. Pascoli, R. de Lima and L. F. Fraceto, Neem Oil and Crop Protection: From Now to the Future, *Front. Plant Sci.*, 2016, **7**, 1–8.
28 V. Sharma and P. P. Kundu, Condensation polymers from natural oils, *Prog. Polym. Sci.*, 2008, **33**(12), 1199–1215.
29 A. Rodriguez-Galan, L. Franco and J. Puiggali, Degradable Poly(ester amide)s for Biomedical Applications, *Polymers*, 2011, **3**(1), 65–99.
30 N. Killi, A. T. Pawar and R. V. N. Gundloori, Polyesteramide of Neem Oil and Its Blends as an Active Nanomaterial for Tissue Regeneration, *ACS Appl. Bio Mater.*, 2019, **2**(8), 3341–3351.
31 Y. X. Dong, S. Liao, M. Ngiam, C. K. Chan and S. Ramakrishna, Degradation Behaviors of Electrospun Resorbable Polyester Nanofibers, *Tissue Eng., Part B*, 2009, **15**(3), 333–351.
32 A. Rahman and F. A. Talukder, Bioefficacy of some plant derivatives that protect grain against the pulse beetle, *Callosobruchus maculatus*, *J. Insect Sci.*, 2006, **6**, 1–10.
33 X. X. Wang, C. Pellerin and C. G. Bazuin, Enhancing the Electrospinnability of Low Molecular Weight Polymers Using Small Effective Cross-Linkers, *Macromolecules*, 2016, **49**(3), 891–899.
34 A. Mohamed, V. L. Finkenstadt, S. H. Gordon, G. Biresaw, P. Debra and P. Rayas-Duarte, Thermal Properties of PCL/Gluten Bioblends Characterized by TGA, DSC, SEM, and Infrared-PAS, *J. Appl. Polym. Sci.*, 2008, **110**(5), 3256–3266.
35 S. Gautam, A. K. Dinda and N. C. Mishra, Fabrication and characterization of PCL/gelatin composite nanofibrous scaffold for tissue engineering applications by electrospinning method, *Mater. Sci. Eng., C*, 2013, **33**(3), 1228–1235.
36 J. Natarajan, D. Queeny, S. N. Shetty, K. Sarkar, G. Madras and K. Chatterjee, Poly(ester amide)s from Soybean Oil for Modulated Release and Bone Regeneration, *ACS Appl. Mater. Interfaces*, 2016, **8**(38), 25170–25184.
37 N. D. Gershon, K. R. Porter and B. L. Trus, The cytoplasmic matrix: Its volume and surface area and the diffusion of molecules through it, *Proc. Natl. Acad. Sci. U. S. A.*, 1985, **82**(15), 5030–5034.